A two-anode reduction technique to monitor the defect and dope the surface of TiO$_2$ nanotube array as photo-anode for water splitting

Xuelan Hou[a],[1], Shaohong Jiang[a], Yongdan Li[a],[b],*

[a] Collaborative Innovation Center of Chemical Science and Engineering (Tianjin), Tianjin Key Laboratory of Applied Catalysis Science and Technology, State Key Laboratory of Chemical Engineering, Tianjin University, Tianjin 300072, China
[b] Department of Chemical and Metallurgical Engineering, School of Chemical Engineering, Aalto University, Kemistintie 1, Espoo, P. O. Box 16100, FI-00076 Aalto, Finland

ARTICLE INFO

ABSTRACT

A two-anode reduction (TAR) technique is adopted to prepare, in one step without the existence of gaseous hydrogen, black TiO$_2$ nanotubes co-doped with carbon and nitrogen. A sample prepared with the TAR technique for 2 min achieved the highest photocurrent response as 2.05 mA/cm^2, which is 3 times as high as that of the pristine TiO$_2$ nanotubes. A synergistic effect between black hydrogenation and C, N co-doping is observed. The light absorption in the whole ultraviolet-visible (UV–vis) range is also greatly enhanced.

1. Introduction

As the earliest discovered and the most intensively investigated semiconductor for photoelectrochemical (PEC) water splitting, TiO$_2$ is still an interesting material due to its low cost, non-toxicity and high stability. In recent two decades, one-dimensional TiO$_2$ nanotube array has been one of the focuses in the exploration of photo-anode materials for water splitting, due to its high surface-to-volume ratio and size dependent property resulting from the large specific surface area and well-defined configuration [1,2]. However, the wide bandgap of pristine TiO$_2$ (typically 3.0–3.2 eV) is still a great challenge in the solar energy harvesting [3]. An enormous amount of approaches has been proposed to narrow the bandgap of TiO$_2$ and limit the recombination rate of the photo-generated electrons and holes to improve the activity of TiO$_2$ as the anode in PEC water splitting [4–6].

One of the approaches has been doping with metallic and non-metallic atoms. Dong et al. [7] prepared Ni-doped TiO$_2$ nanotubes by an anodization method with Ti-Ni alloy (1 wt.% Ni and 10 wt.% Ti). Compared with the undoped TiO$_2$, the absorption edge of the Ni-doped samples showed an enhancing red shift with the increase of the Ni-doping amount. The highest photocurrent response of Ni-doped TiO$_2$ nanotubes was 0.85 mA/cm^2, while the undoped TiO$_2$ showed 0.40 mA/cm^2. Liu et al. [8] fabricated C-N co-doped TiO$_2$ nanotube /carbon nanorod composite by chemical vapor deposition [8]. Molla-vali et al. [9] employed a one-step anode oxidation technique, and K$_2$

[Ni (CN)$_4$] as the source of dopant to prepare C, N and Ni co-doped TiO$_2$ nanotubes. The photocurrent density of the un-doped TiO$_2$ and co-doped TiO$_2$ nanotubes were 13.78 μA/cm^2 and 143 μA/cm^2 under visible light irradiation. Very recently, Georgieva et al. [4] reported that co-doping of B and N into TiO$_2$ nanotubes also led to a remarkable photocurrent enhancement.

In parallel to the effort of doping TiO$_2$ nanotubes, reducing TiO$_2$ is another interesting technique. Chen et al. [10] firstly kept the TiO$_2$ white powder in vacuum for 1 h and then annealed the sample in 2.0 MPa H$_2$ atmosphere at around 200 °C for 5 days to get black TiO$_2$ nanoparticals, which exhibited a bandgap of around 1.0 eV with a greatly enhanced photocatalytic activity in powder photo-catalytic water splitting. After Chen's work, hydrogen treatment to get blackened TiO$_2$ material becomes one of the important techniques in the preparation of TiO$_2$ photoanode material [11–14]. Wang et al. [15] utilized a hydrogen plasma, 200 W input power for 4–8 h at 500 °C, to prepare a core/shell structured TiO$_2$@TiO$_{2-x}$H$_x$ sample. Zhou et al. [16] reported a procedure to get ordered mesoporous black TiO$_2$. Firstly, the sample was annealed at 350 °C under N$_2$ for 3 h and then calcined at 700 °C in air for 2 h. After the cooling down of oven to 200 °C, it was switched to N$_2$ for 0.5 h to remove air. Finally, the sample was annealed in H$_2$ flow under normal pressure for 3 h at 500 °C. Islam et al. [6] adopted a sol-gel and hydrogen plasma doping route to get blackened TiO$_2$ thin film and observed an enhanced light absorption from UV to almost the whole visible light range. Liu et al. [11] utilized a high-

energy proton ion-implantation method to introduce defects to form "black" TiO_2 nanotubes. They also prepared black TiO_2 nanotubes with annealing in H_2 with a pressure of 2.0 MPa at 500 °C for 1 h [17].

Up to date, the synthesis techniques of blackened TiO_2 mostly involve an extra hydrogen source, and most of the preparation methods are complex and need long time. Herein, we report a novel, safe and simple technique to blacken TiO_2 nanotube without the involvement of extra gaseous hydrogen, which also enables doping of C and N simultaneously into the TiO_2 nanotubes.

2. Experimental

2.1. Materials

Titanium foil (Ti, purity 99.5%, thickness 0.02 cm, Beijing Zhongnuo Advanced Material Technology Co., Ltd), ethylene glycol ($C_2H_6O_2$, > 99%, Shanghai Aladdin Industrial Corporation), ammonium fluoride (NH_4F, AR, Tianjin Guangfu Technology Development Co., Ltd), sodium hydroxide (NaOH, AR, Tianjin Guangfu Technology Development Co., Ltd) and graphite rods (99.99%, diameter, D = 0.6 cm, length = 10.0 cm, Beijing HWRK Chem Co.). All the materials were used without further treatment. The aqueous solutions were prepared with deionized (DI) water.

2.2. Preparation of samples

Prior to the anodization, Ti foils (1.0×2.0 cm) were ultrasonically cleaned with acetone, ethanol and deionized (DI) water sequentially and dried in a vacuum furnace at 70 °C. The anodic oxidation was carried out with a two-electrode configuration with a Ti foil as the anode and a Pt sheet as the counter electrode in the electrolyte, which is a mixture of 0.3 wt.% NH_4F and 6 vol% H_2O in ethylene glycol (EG) under a voltage of 60 V for 3 h at room temperature [17,18]. After that, the formed TiO_2 nanotube array is anodic TiO_2 nanotubes (Fig. 1(a)). Then, the anodic TiO_2 nanotube array is annealed at 450 °C for 30 min with a ramping rate of 5 °C/min in the muffle oven under air atmosphere, after which the TiO_2 nanotube sample is denoted as NT. As shown in Fig. 1(b), the NT sample is treated with a two-anode reduction (TAR) technique in a three-electrode device with a Ti foil (1.0×2.0 cm) and a graphite rod as the anodes, while the NT sample as the cathode. The electrolyte solution and voltage are the same as those in the anodization process, respectively. After TAR treatment for a specific time period, i.e. 1, 2 and 3 min, respectively for three samples, black colored intermediate TiO_2 nanotube array is formed. Finally, the black intermediate sample is annealed again at 450 °C for 30 min with a ramp of 5 °C/min in the muffle oven in air. The final samples are referred to as TAR-x, where x is the time in min.

2.3. Photoelectrochemical measurements

PEC measurement was carried out with an electrochemical workstation CHI 660B in a three-electrode device with platinum (Pt) as the counter electrode and Ag/AgCl as the reference electrode. The TAR sample was irradiated under AM 1.5 simulated sunlight from a xenon lamp (Perfect Light, PLS-SXE-300). The surface area of the sample under irradiation and in contact with the electrolyte (1.0 M NaOH) was 1.0 cm^2.

2.4. Characterization

The morphology was observed with a field-emission scanning electron microscope (SEM; FEI, Nanosem-430) and a transmission electron microscope (TEM; JEOL, JEM-2100 F, exited at 120 kV). The X-ray photoelectron spectroscopy (XPS) analysis was carried out using a PHI 5000 VersaProbe with an Mg-Kα X-ray excitation source. The FT-IR spectrum was recorded using a Perkin-Elmer FT-IR spectrometer. The ultraviolet-visible (UV–vis) diffuse reflection spectra were acquired with a PerkinElmer Lambda 750S equipment. The photoluminescence (PL) spectra excited at 330 nm was measured from 340 nm to 600 nm with a Jobin-Yvon-Fluorolog 3–21 spectrofluorimeter at room temperature. Ultraviolet photoemission spectroscopy (UPS) was measured on Perkin Elmer PHI 3057 XPS system. The excitation source was He I line (hν = 21.21 eV).

3. Results

3.1. Phenomenon during the TAR process

A constant voltage of 60 V was applied in the TAR device. A large amount of gas bubbles was released on the cathode surface. That is because a large amount of H^+ together with NH_4^+ in EG solution move to the surface of the cathode, where it is reduced to H and released as H_2 and NH_3. The surface newly formed H_2 is very reductive and thus blackens the TiO_2 nanotubes quickly to form a black intermediate TiO_2 nanotube array. However, the H^+ on the cathode surface also etches the surface at a 60 V applied voltage.

3.2. Photo-electro-chemical performance

The photocurrent densities of the samples are plotted in Fig. 2(a). The NT, TAR-1, TAR-2 and TAR-3 samples give responses as 0.71, 1.44, 2.05 and 1.73 mA/cm^2, respectively at a bias of 0.6 V (vs. Ag/AgCl).
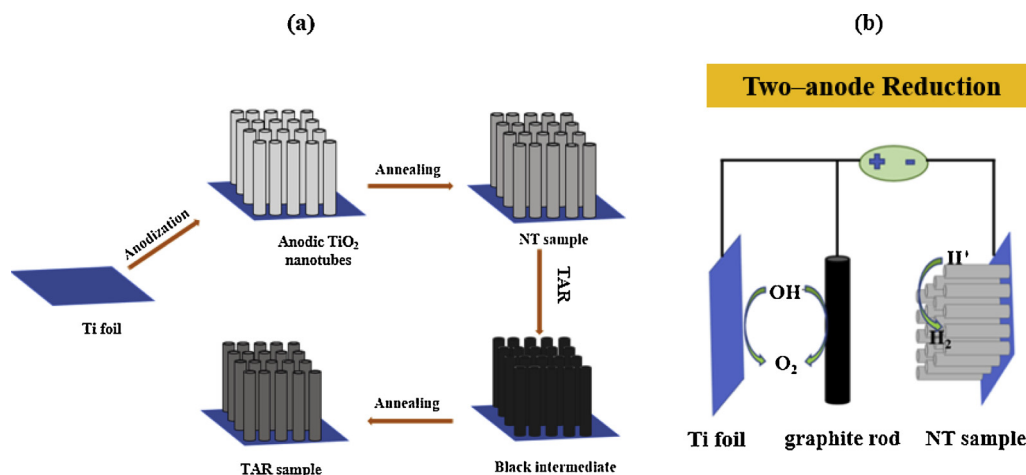
(a)　　　　　　　　　　　　　　　　　　　　**(b)**

Fig. 1. (a) The schematic diagram of the preparation process of TAR sample, (b) The schematic diagram of the TAR device.
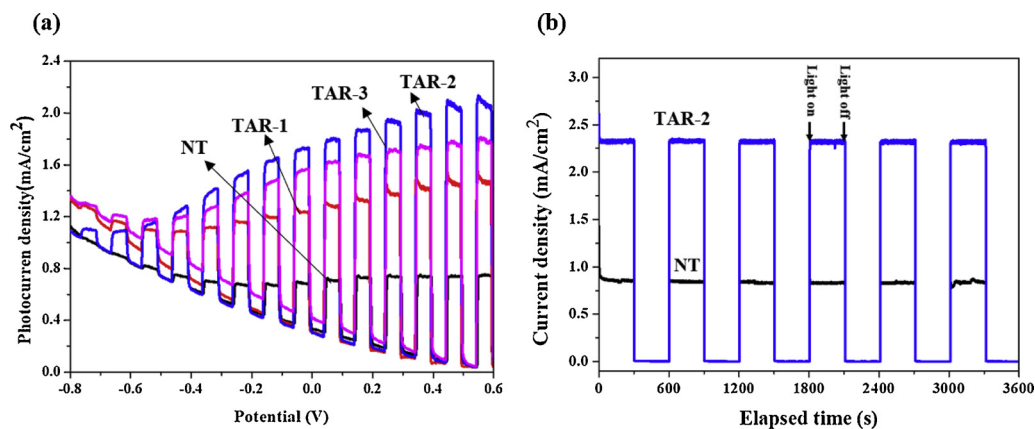
Fig. 2. (a) Polarization curves of the samples of NT, TAR-1, TAR-2 and TAR-3 with a scan rate of 5 mV/s from -0.8 V to 0.6 V (vs. Ag/AgCl). (b) The intermittent photocurrent density-time curves of the samples of NT and TAR-2 in light on-off cycles at an applied bias of 0.6 V (vs. Ag/AgCl).

Compared to that of the NT sample, TAR-2 achieves the highest enhancement, nearly 3 times as high as that of NT at the specific bias potential. When the TAR time is 3 min, the sample gives a lowered photocurrent. Fig. 2(b) illustrates the time-resolved photocurrent response of NT and TAR-2 samples under the same illuminating condition. When the light is turned on, the current density increases vertically and when the light irradiation is turned off, the current presents a sharp decrease, which means that the carrier transfer happens instantly. In 3600 s, the performance of the two samples keeps stable.

3.3. Catalyst characterization

Fig. 3 gives the surface micrographs of the NT and TAR-2 samples. The TiO_2 nanotubes are open on the top and vertically aligned. Both samples are arranged in tight bundles without connection between each other. The number of TiO_2 nanotubes in 1.0 cm^2 is roughly 6.9*10^9. The average inner diameters both are around 115 nm, and the average lengths of the nanotubes are both 14.1 μm in the two samples. However, TAR leads to the decoration of nanoparticles on the out surface of the tubes, as shown in Fig. 3(c). The TEM images in Fig. 4(a) and (b), reveal some more differences between the two samples. The TAR-2 sample shows distribution of particles with size around 10 nm on the out surface of the tubes, while the NT sample gives a smooth surface. The HRTEM micrographs show further that TiO_2 in NT sample is highly crystallized with clear lattice fringes in Fig. 4(c). The TAR-2 sample in Fig. 4(d) also exhibits clear lattice fringes in most part of the window. However, the sample does have amorphous domains with unclear lattice fringes as highlighted with the white circles [18,19]. The amorphous areas are regard as the defected parts in the crystal bulk [18]. Although we used a graphite rod as one of the anodes in TAR device,
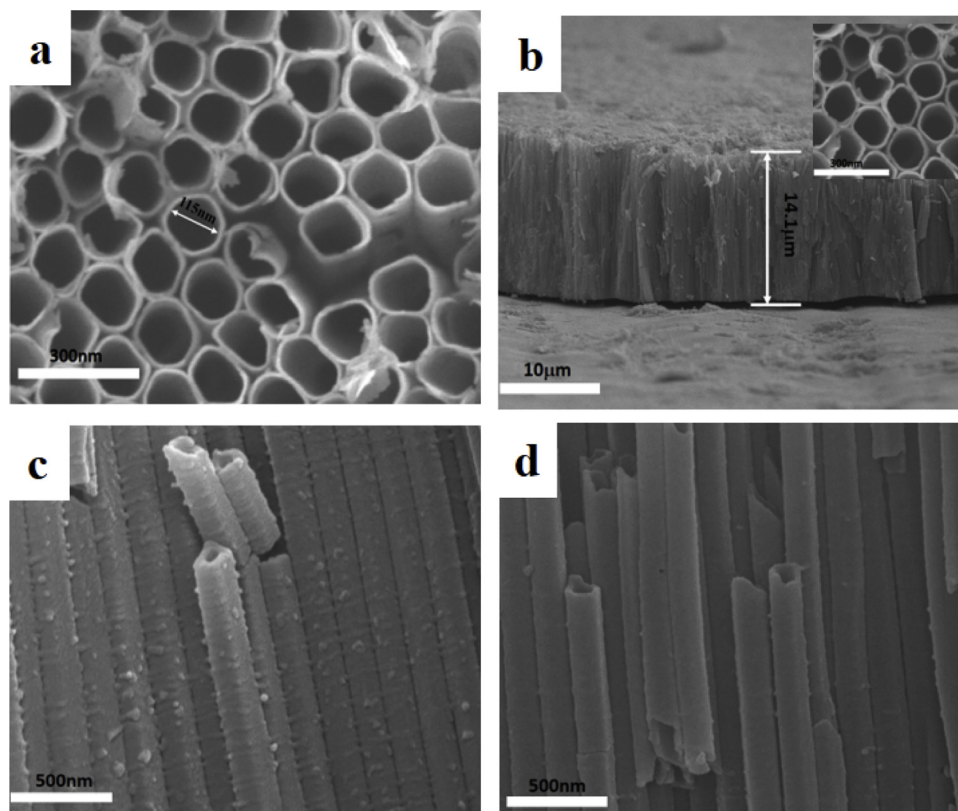

Fig. 3. (a) The top surface views of TAR-2, the cross-sectional views of the samples (b) NT, (c) TAR-2 and (d) NT.
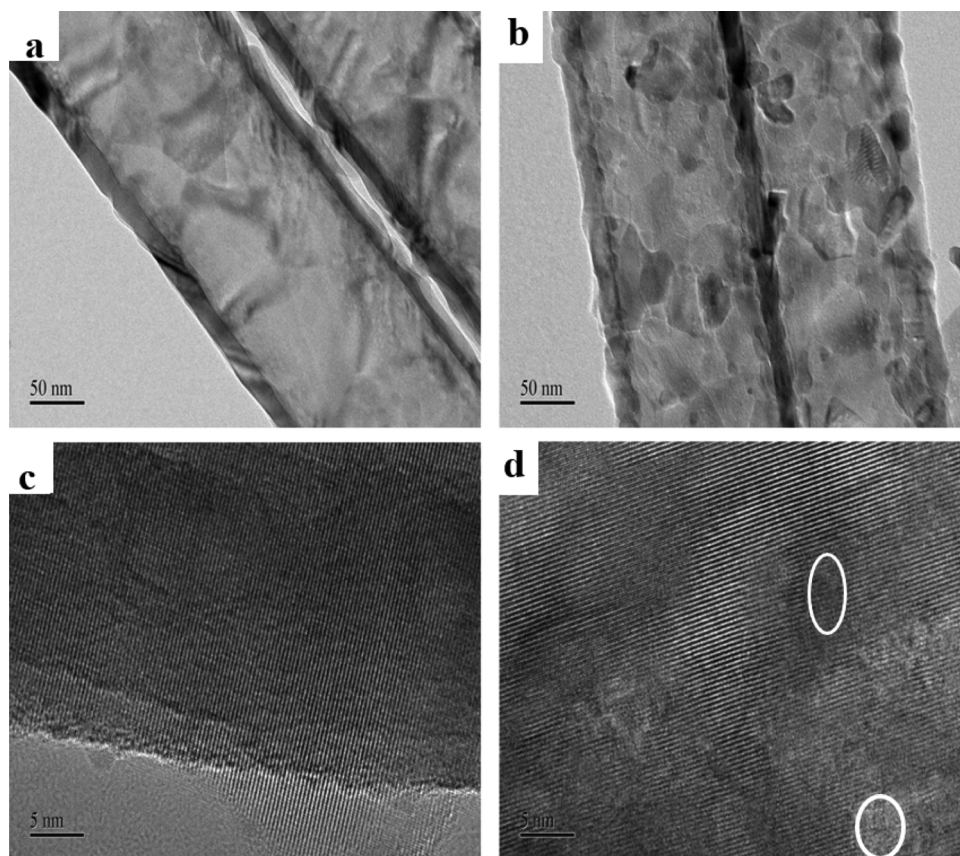
Fig. 4. TEM images (a) NT, (b) TAR-2, and HRTEM micrographs (c) NT, (d) TAR-2.

carbon quantum dots are not observed in the TEM images.

In Fig. 5(a), the C 1s spectrum of NT sample, the XPS peak at around 285.9 eV corresponds to the band of C-O H [20]. The peak at 287 eV is the binding energy of C−O bond, while a shift of 0.7 eV to the higher end suggests the presence of C=O [21]. In Fig. 5(b), TAR-2 sample shows two extra peaks at 283.6 eV and 289.7 eV in the C 1s XPS spectrum. The peak at 283.6 eV corresponds to the binding energy of Ti-C [20,22], and that at 289.7 eV represents the carbonate (CO_3^{2-}) [23,24]. In the N 1s spectrum, Fig. 5(c), the peak at 397.5 eV is the binding energy of Ti-N bond [25]. Because NH_3 absorbs on the surface, a peak appears at 401 eV [25]. The peak at 404.6 eV is speculated to be representative of NO_3- or -NO_2 [26], which appears only in the spectrum of the TAR

sample. These results indicate that C and N are chemically incorporated into the TiO_2 in the TAR process. For the O 1s XPS spectrum, Fig. 5(e), the peak at 530.5 eV and 531.0 eV are assigned to lattice oxygen (O_L) and hydroxyl oxygen (O−H) [9]. In Fig. 5(f), the new peak at 531.8 eV is attributed to the bond of O to C or N for forming carbonate or oxynitride [25,27]. From the XPS results, it is informed that, in the TAR treatment, Ti-C and Ti-N bonds form, and OH-, COOH- and CO_3^{2-} groups anchor on the surface of TAR-2.

In Fig. 6(a), both samples show similar absorption bands in their FT-IR spectra in the range of 4000-400 cm^{-1}. The band at around 520 cm^{-1} is related to the Ti–O bond [18]. The absorption at around 1630 cm^{-1} is due to C=O in carboxyl groups [28]. The peak at around
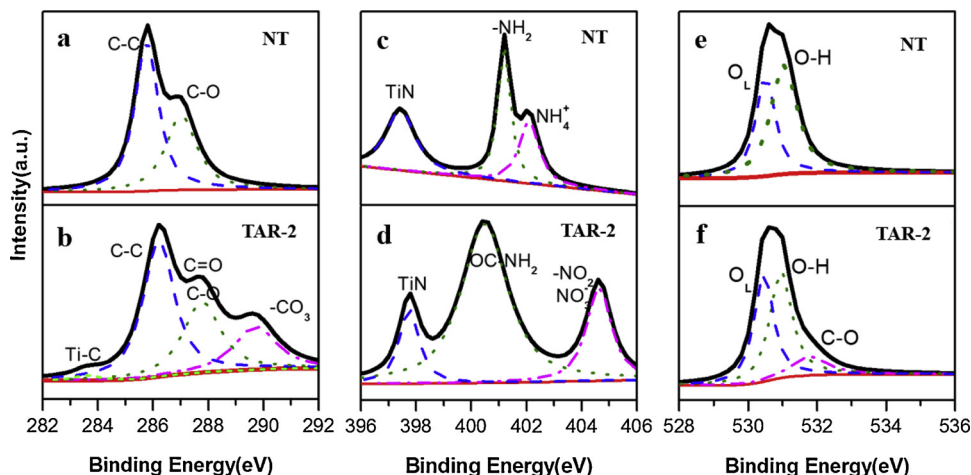

Fig. 5. The XPS spectra of the C 1s of the samples of NT and TAR-2, (a) and (b); N1s of the samples of NT and TAR-2, (c) and (d); O 1s of the samples of NT and TAR-2, (e) and (f).
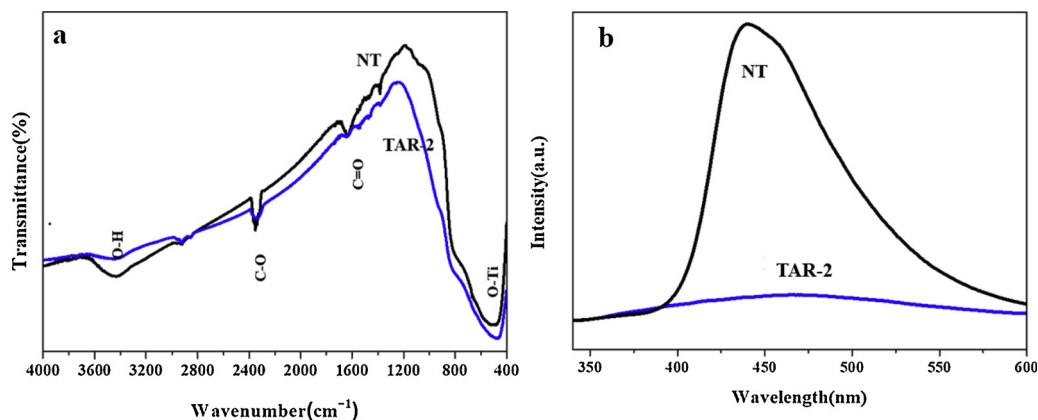
Fig. 6. (a) The FT-IR spectra, (b) Photoluminescence spectra of NT and TAR-2 samples.

$2345\,cm^{-1}$ is attributed to the stretching of C−O bond [29,30]. Compared to the spectrum of NT sample, TAR-2 shows a widened absorption at around $3460\,cm^{-1}$, which is assigned to O−H stretching by Chen et al. [28,31], to the hydrogen incorporation into the TiO_2 nanotubes. As illustrated in Fig. 6(b), the PL intensity of TAR-2 sample exhibits a remarkable decrease than that of the NT sample. The PL spectra is often used to evaluate the separation and utilization efficiency of the photo stimulated electrons (e-) and holes (h^+) [32,33]. The result indicates that after TAR treatment the separation and utilization efficiency of the e- and h^+ pairs are effectively enhanced.

The UV–vis absorption spectra of the two samples are depicted in Fig. 7(a). TAR-2 sample shows absorption in the entire range of solar spectrum, while the NT sample only shows absorption in the UV range. The NT sample has an absorption edge at 387 nm [27]. The absorption of the TAR-2 sample splits into two edges at 449 and 626 nm, respectively, meaning that the TAR treatment broadens the absorption region and forms a mid-gap. The UV–vis absorption intensity of TAR-2 at 800 nm is as high as absorption intensity of NT sample at 300 nm. The Tauc plots were derived as Fig. 7(b), and a major bandgap of 2.81 eV was formed with an extra mid-gap of 1.78 eV.

As illustrated in Fig. 8, the secondary-electron cut off energy of sample NT and TAR-2 are located at 17.47 eV and 17.66 eV, respectively. Electron binding energy is calculated with respect to the Fermi level. The work function ($\Phi = h\nu - E_{cut-off}$) values are 3.74 eV for NT sample and 3.55 eV for TAR-2 sample, respectively. The insert figure is the valence band maximum of the NT and TAR-2 samples, which are 3.34 eV and 3.42 eV corresponding to the Fermi levels, respectively. Both them also show valence band tail states, at 1.80 eV and 1.67 eV, respectively.
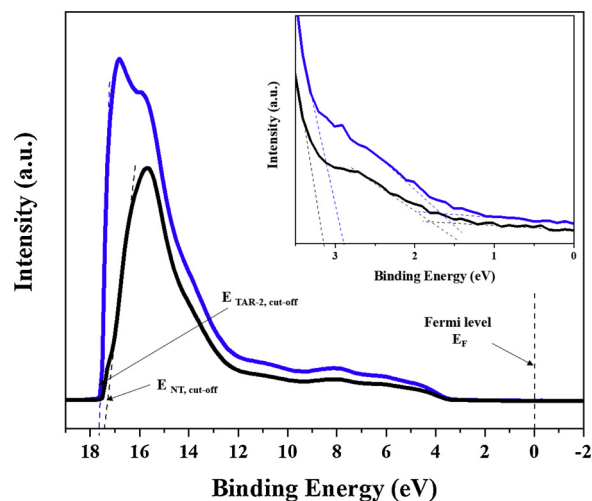

Fig. 8. UPS spectra of NT sample and TAR-2 sample.

4. Discussion

Both the reduction and doping affect the light absorption. However, the doping method mostly shifts the absorption edge, while the reduction method also broadens the light absorption range. It has been already reported that the black hydrogenated TiO_2 nanocrystals broadened the light absorption to about 1200 nm vavelength [10]. For instance, Ren et al· [34] adopted a high-power density H_2 plasma to prepare H-TiO_2 nanoparticles and also showed an enhanced ultraviolet-visible-near infrared light absorption. The C and N doping shifts the
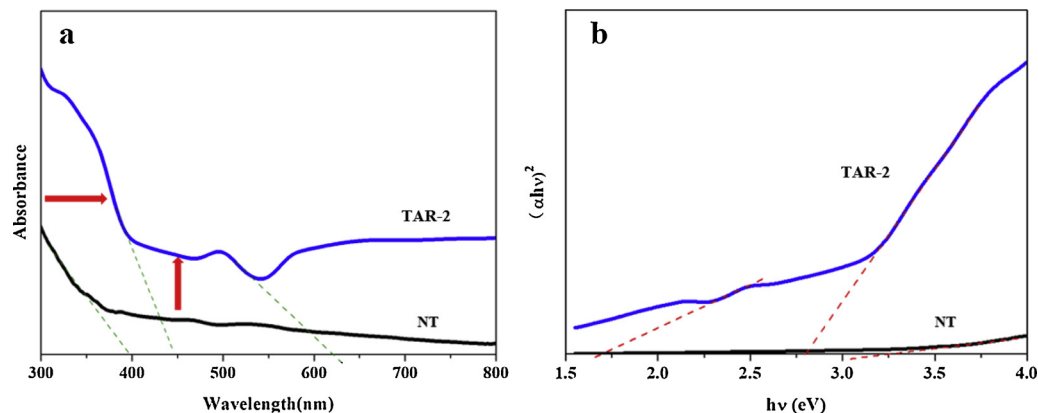

Fig. 7. (a) UV–vis absorption spectra, (b) The derived Tauc plots of the NT and TAR-2 samples.

TAR-2

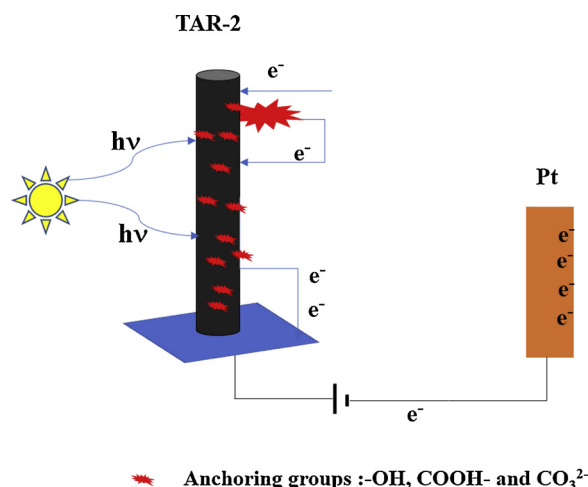**⚹ Anchoring groups :-OH, COOH- and CO₃²⁻**

Fig. 9. Scheme of the electron transfer path in TAR-2 photoanode in PEC water splitting.

absorption edge. Most of the reported works on doping also showed the enhancement of the light absorption in the range of 300 nm–600 nm, and the absorption goes close to zero at the end of the absorption spectra, around 700 nm–800 nm [35–38].

As we know, anchoring groups have strong effect on the nature of conduction and the energy levels of the related bands affecting their donor and acceptor properties [39]. To clarify the electronic and photonic effect of the anchoring groups on TAR-2 in water splitting, a schematic diagram of electron transfer path on TAR-2 photoanode in water splitting is illustrated as Fig. 9. As shown in the diagram, when the light irradiates on the surface, not only the TiO_2 nanotubes, but also the anchoring groups (-OH, COOH- and CO_3^{2-}) absorb photons from the light. When the TiO_2 nanotubes absorb the photons, the electrons are excited to the conduction band, then flow to the Ti foil, and transfer through the external load or to be utilized to produce H_2. When the electrons in the functional groups get excited, they transfer to the semiconductor. The functional groups on the TAR sample enhances the lifetime of the electrons. It is noted that COOH- and CO_3^{2-} have π orbitals, which may act as electron transfer channels to accelerate the electron transfer to the cathode.

5. Conclusion

A TAR technique is adopted to promote the performance of TiO_2 nanotube array as the photoanode in water splitting. The sample treated in TAR device at 60 V in room temperature for 2 min gives the highest photo-current response 2.05 mA/cm², in 1 M NaOH under AM1.5 simulated sunlight, which is nearly 3 times of NT sample, while the NT and TAR-2 samples have the same diameter (115 nm) and tube length (14.1 μm). XPS measurement results show the evidence that C and N are co-doped into the surface layer of the TiO_2 nanotubes. FT-IR spectra give further evidence for the C and N co-doping, and indicate that hydrogen atoms are incorporated into the TiO_2 lattice during the TAR treatment. C, N and H form on the surface functional groups like -OH, COOH- and CO_3^{2-}. The anchored groups enhance electron transfer and light absorption. Blackening and C and N co-doping of the TiO_2 nanotubes have a synergy effect to enhance the UV–vis light absorption. The light absorption of TAR-2 is confirmed to be effectively enhanced in the whole range from UV to visible light. The UV–vis absorption intensity of TAR-2 at 800 nm is similar as that of the NT sample at 300 nm. The PL spectrum indicates that the separation efficiency of photogenerated carriers are greatly improved after the TAR treatment.

Appendix A. Supplementary data

Supplementary material related to this article can be found, in the online version, at doi:https://doi.org/10.1016/j.apcatb.2019.117949.

References

[1] Z. Jiang, F. Yang, N.J. Luo, B.T.T. Chu, D.Y. Sun, H.H. Shi, T.C. Xiao, P.P. Edwards, Solvothermal synthesis of N-doped TiO₂ nanotubes for visible-light-responsive photocatalysis, Chem. Commun. (2008) 6372–6374.

[2] R. Asahi, T.M.T. Ohwaki, K. Aoki, Y. Taga, Visible light photocatalysis in nitrogen-doped titanium oxides, Science 293 (2001) 269–271.

[3] X. Li, J.G. Yu, J.X. Low, Y.P. Fang, J. Xiao, X.B. Chen, Engineering heterogeneous semiconductors for solar water splitting, J. Mater. Chem. A 3 (2015) 2485–2534.

[4] J. Georgieva, E. Valova, S. Armyanov, D. Tatchev, S. Sotiropoulos, I. Avramova, N. Dimitrova, A. Hubin, O. Steenhaut, A simple preparation method and characterization of B and N co-doped TiO₂ nanotube arrays with enhanced photoelectrochemical performance, Appl. Surf. Sci. 413 (2017) 284–291.

[5] Z. Wang, C.Y. Yang, T.Q. Lin, Y. Yin, D.Y. Wan, F.F. Xu, F.Q. Huang, X.M. Xie, M.H. Jiang, Visible-light photocatalytic, solar thermal and photoelectrochemical properties of aluminium-reduced black titania, Energy Environ. Sci. 6 (2013) 3007–3014.

[6] S.Z. Islam, A. Reed, S. Nagpure, N. Wanninayake, J.F. Browning, J. Strzalka, D.Y. Kim, S.E. Rankin, Hydrogen incorporation by plasma treatment gives mesoporous black TiO₂ thin films with visible photoelectrochemical water oxidation activity, Microporous Mesoporous Mater 261 (2018) 35–43.

[7] Z.B. Dong, D.Y. Ding, T. Li, C.Q. Ning, Ni-doped TiO₂ nanotubes photoanode for enhanced photoelectrochemical water splitting, Appl. Surf. Sci. (2018) S0169433218306913.

[8] S.H. Liu, L.X. Yang, S.H. Xu, S.L. Luo, Q.Y. Cai, Photocatalytic activities of C-N-doped TiO₂ nanotube array/carbon nanorod composite, Electrochem. Commun. 11 (2009) 1748–1751.

[9] M. Mollavali, C. Falamaki, S. Rohani, Preparation of multiple-doped TiO₂ nanotube arrays with nitrogen, carbon and nickel with enhanced visible light photoelectrochemical activity via single-step anodization, Int. J. Hydrogen Energy 40 (2015) 12239–12252.

[10] X.B. Chen, L. Liu, P.Y. Yu, S.S. Mao, Increasing Solar Absorption for Photocatalysis with black hydrogenated titanium dioxide nanocrystals, Science 331 (2011) 746–750.

[11] N. Liu, V. Haublein, X.M. Zhou, U. Venkatesan, M. Hartmann, M. Mackovic, T. Nakajima, E. Spiecker, A. Osvet, L. Frey, P. Schmuki, "Black" TiO₂ nanotubes formed by high-energy proton implantation show noble-metal-co-catalyst free photocatalytic H₂evolution, Nano Lett. 15 (2015) 6815–6820.

[12] J.M. Cai, Y.M. Zhu, D.S. Liu, M. Meng, Z.P. Hu, Z. Jiang, Synergistic effect of titanate-anatase heterostructure and hydrogenation-induced surface disorder on photocatalytic water splitting, ACS Catal. 5 (2015) 1708–1716.

[13] X.D. Wang, S. Estrade, Y.J. Lino, F. Yu, L. Lopez-Conesa, H. Zhou, S.K. Gurramb, F. Peiro, Z.Y. Fan, H. Shen, L. Schaefer, G. Braeuer, A. Waagi, Enhanced photoelectrochemical behavior of H-TiO₂ nanorods hydrogenated by controlled and local rapid thermal annealing, Nanoscale Res. Lett. 12 (2017) 336.

[14] L. Liu, X.B. Chen, Titanium dioxide nanomaterials: self-structural modifications, Chem. Rev. 14 (2014) 9890–9899.

[15] Z. Wang, C.Y. Yang, T.Q. Lin, H. Yin, P. Chen, D.Y. Wan, F.F. Xu, F.Q. Huang, J.H. Lin, X.M. Xie, M.H. Jiang, H-doped black titania with very high solar absorption and excellent photocatalysis enhanced by localized surface plasmon resonance, Adv. Funct.Mater 23 (2013) 5444–5450.

[16] W. Zhou, W. Li, J.Q. Wang, Y. Qu, Y. Yang, Y. Xie, K.F. Zhang, L. Wang, H.G. Fu, D.Y. Zhao, Ordered mesoporous black TiO₂ as highly efficient hydrogen evolution photocatalys, J. Am. Chem.Soc. 136 (2014) 9280–9283.

[17] N. Liu, C. Schneider, D. Freitag, M. Hartmann, U. Venkatesan, J. Muller, E.Spiecker, P. Schmuki, Black TiO₂ Nanotubes: Cocatalyst-free open-circuit hydrogen generation, Nano Lett. 14 (2014) 3309–3313.

[18] S.G. Ullattil, P. Periyat, A 'one pot' gel combustion strategy towards Ti³⁺ self-doped 'black' anatase TiO₂₋ₓ solar photocatalyst, J. Mater. Chem. A 4 (2016) 5854–5858.

[19] T. Jedsukontorn, T. Ueno, N. Saito, M. Hunsom, Narrowing band gap energy of defective black TiO₂ fabricated by solution plasma process and its photocatalytic activity on glycerol transformation, J. Alloys Compd. 757 (2018) 188–199.

[20] Y. Huang, W.K. Ho, S.C. Lee, L.Z. Zhang, G.S. Li, J.C. Yu, Effect of carbon doping on the mesoporous structure of nanocrystalline titanium dioxide and its solar-light-

driven photocatalytic degradation of NOx, Langmuir 24 (2008) 3510–3516.

[21] D. Yang, A. Velamakanni, G. Bozoklu, S. Park, M. Stoller, R.D. Piner, S. Stankovich, I. Jung, D.A. Field, C.A. Ventrice, R.S. Ruoff, Chemical analysis of graphene oxide films after heat and chemical treatments by X-ray photoelectron and Micro-Raman spectroscopy, Carbon 47 (2009) 145–152.

[22] L.C. Chen, Y.C. Ho, W.S. Guo, C.M. Huang, T.C. Pan, Enhanced visible light-induced photoelectrocatalytic degradation of phenol by carbon nanotube-doped TiO_2 electrodes, Electrochim. Acta 54 (2009) 3884–3891.

[23] D. Lawless, S. Kapoor, D. Meisel, Bifunctional capping of CdS nanoparticles and bridging to TiO_2, J. Phys. Chem. C 99 (1995) 10329–10335.

[24] T. Ohno, T. Tsubota, K. Nishijima, Z. Miyamoto, Degradation of methylene blue on carbonate species-doped TiO_2 photocatalysts under visible light, Chem. Lett. 33 (2004) 750–751.

[25] F. Peng, L.F. Cai, H. Yu, H.J. Wang, J. Yang, Synthesis and characterization of substitutional and interstitial nitrogen-doped titanium dioxides with visible light photocatalytic activity, J. Solid State Chem. 181 (2018) 130–136.

[26] J.P. Shen, X.H. Duan, Q.P. Luo, Y. Zhou, Q.L. Bao, Yj. Ma, C.H. Pei, Preparation and characterization of a novel cocrystal explosive, Cryst. Growth Des. 11 (2011) 1759–1765.

[27] Y.P. Peng, H.L. Chen, C.P. Huang, The synergistic effect of photoelectrochemical (PEC) reactions exemplified by concurrentperfluorooctanoic acid (PFOA) degradation and hydrogen generation over carbon and nitrogen codoped TiO_2 nanotube arrays (C-N-TNTAs) photoelectrode, Appl. Catal. B: Environ. 209 (2017) 437–446.

[28] X. Zhang, F. Wang, H. Huang, H.T. Li, X. Han, Y. Liu, Z.H. Kang, Carbon quantum dot sensitized TiO_2 nanotube arrays for photoelectrochemical hydrogen generation under visible light, Nanoscale 5 (2013) 2274.

[29] M.I. Baraton, L. Merhari, Advances in air quality monitoring via nanotechnology, J. Nanopart. Res. 6 (2014) 107–117.

[30] A. Phlayrahan, N. Monarumit, S. Satitkune, P. Wathanakual, Role of Ti content on the occurrence of the $3309\text{-}cm^{-1}$ peak in FTIR absorption Spectra of Ruby Samples, J. Appl. Spectrosco. 85 (2018) 385–390.

[31] X.B. Chen, L. Liu, Z. Liu, M.A. Marcus, W.C. Wang, N.A. Oyler, M.E. Grass, B.H. Mao, P.A. Glans, P.Y. Yu, J.H. Guo, S.S. Mao, Properties of disorder-engineered black titanium dioxide nanoparticles through hydrogenation, Sci. Rep. 3 (2013) 1510 —.

[32] S.H. Jiang, Y. Li, X.L. Zhang, Y.D. Li, Enhancing the photoelectrochemical water splitting activity of rutile nanorods by removal of surface hydroxyl groups, Catal. Today 259 (2016) 360–367.

[33] Y. Li, X.L. Zhang, S.H. Jiang, H.T. Dai, X.W. Sun, Y.D. Li, Improved photoelectrochemical property of a nanocomposite NiO/CdS@ZnO photoanode for water splitting, Sol. Energy Mater. Sol. C 132 (2015) 40–46.

[34] W.Z. Ren, Y. Yan, L.Y. Zeng, Z.Z. Shi, A. Gong, P. Schaaf, D. Wang, J.S. Zhao, B.B. Zou, H.S. Yu, G. Chen, E.M.B. Brown, A.G. Wu, A near infrared light triggered hydrogenated black TiO_2 for cancer photothermal therapy, Adv. Healthcare Mater. 4 (2015) 1526–1536.

[35] X.X. Yang, C.D. Cao, L. Erickson, K. Hohn, R. Maghirang, K. Klabunde, Photo-catalytic degradation of rhodamine B on C-, S-, N-, and Fe-doped TiO_2 under visible-light irradiation, Appl. Catal. B: Environ. 91 (2009) 657–662.

[36] F. Dong, W.R. Zhao, Z.B. Wu, Characterization and photocatalytic activities of C, N and S co-doped TiO_2, with 1D nanostructure prepared by the nano-confinement effect, Nanotechnology 19 (2008) 365607.

[37] G.S. Zhang, Y.C. Zhang, M. Nadagouda, C. Han, K. O'Shea, S.M. El-Sheikh, A.A. Ismail, D.D. Dionysiou, Visible light-sensitized S, N and C co-doped polymorphic TiO_2 for photocatalytic destruction of microcystin-LR, Appl. Catal. B: Environ. 144 (2014) 614–621.

[38] J.J. Jiang, Z.P. Xing, M. Li, Z.Z. Li, X.Y. Wu, M.Q. Hu, J.F. Wan, N. Wang, A.S. Besov, W. Zhou, Insitu Ti^{3+}/N-Codoped three-dimensional (3D) urchinlike black TiO_2 architectures as efficient visible-light-driven photocatalysts, Ind. Eng. Chem. Res. 56 (2017) 7948–7956.

[39] L.A. Zotti, T. Kirchner, J.C. Cuevas, F. Pauly, T. Huhn, E. Scheer, A. Erbe, e, Revealing the role of anchoring groups in the electrical conduction through single-molecule junctions, Small 6 (2010) 1529–1535.